JOURNAL OF AGRICULTURAL AND FOOD CHEMISTRY

Density and Microviscosity Studies of Palm Oil/Water Emulsions

JUAN CARLOS ARBOLEYA, LESLIE H. SUTCLIFFE, AND PETER J. WILDE*

Institute of Food Research, Colney Lane, Norwich Research Park, Norwich, NR4 7UA, United Kingdom

SHIRLEY A. FAIRHURST

John Innes Centre, Colney Lane, Norwich Research Park, NR4 7UH, United Kingdom

Electron paramagnetic resonance (EPR) and densitometry were used to measure the temperature- and rate-dependent formation of fat crystals in emulsion droplets in hardened palm kernel oil in water emulsions. The solid fat content in emulsions can be critical for the functionality of the emulsions in a wide variety of applications. Therefore, new and accessible methods are needed to monitor solid fat content in order to control the functional properties of these emulsions. EPR measurements showed that the microviscosity within the oil droplets could be measured as a function of temperature and that the storage temperature below the main fat melting point is crucial for an increase in the microviscosity, due to fat solidification. The microviscosity of the oil droplets could be an important parameter for defining functional performance (e.g., rheology and partial coalescence). Density measurements provided a simple and accurate method for monitoring changes in phase state of the oil. The phase behavior agreed well with the EPR results, demonstrating that accurate density measurements could prove to be a valuable tool for monitoring fat crystallization processes.

KEYWORDS: Emulsions; density; microviscosity; spin probes; EPR

INTRODUCTION

Oil in water emulsions are utilized in a huge variety of applications including food, cosmetics, pharmaceuticals, and petrochemical industries, and they are used primarily to suspend fat or fat soluble components in an aqueous medium, to impart structure and texture, or to encapsulate aroma or other active compounds for enhanced nutritional quality or drug delivery (*1*, *2*). Physically, the properties of the emulsion droplets themselves can influence the rheological properties of the emulsion as a whole (*3*, *4*). The droplets can form space-spanning networks to create non-Newtonian gellike behavior in order to design the desired rheological properties (*2*, *3*), for example, to retain solidlike behavior during storage but that will flow easily during transport or manipulation. The physical properties of the oil phase of the constituent oil droplets are therefore extremely important for the physical properties of the emulsion network as a whole. That is, a network formed from liquid oil droplets is very different to that formed from solid fat droplets. This effect is utilized in the food industry for the formation of a range of emulsion-based dairy products such as ice cream, whipped cream, and yogurt to enhance the sensory properties of the food (*5*−*7*). It is well-known that the levels of solid fat are vital for the overall appearance, structure, and rheology; therefore, there is a great interest in trying to understand the physicochemical mechanisms underlying the formation of solid fat crystals in oil droplets in order to manipulate the stability, rheology, and functionality of a range of emulsion systems.

The phase behavior of the oil is different in the bulk and emulsified forms. This is thought to be mainly due to the probability that a nucleation site for crystal formation is present in a single emulsified droplet (*3*, *5*, *7*). The impact is that it is possible to supercool emulsion droplets, so that they remain in the liquid phase at temperatures below the main melting point of the fat (*5*, *7*−*12*). On the basis of this premise, the importance of various physicochemical parameters such as droplet size, oil phase, emulsifier type, and droplet interactions has been investigated (*7*−*9*, *13*, *14*), to improve our understanding of how to control the solid fat content of the emulsions and hence influence the functionality of the emulsions themselves. There have been a wide variety of studies on this problem, using a range of techniques (*5*, *7*). These include differential scanning calorimetry (*12*), X-ray diffraction (*15*), NMR (*3*, *10*), volume (*8*), and ultrasound (*9*). These techniques can monitor the rate and extent of crystallization and even the polymorphism of the crystals. The results have often been used to study the problem of heterogeneous vs homogeneous nucleation (*7*). These approaches have revealed a great deal of information about the

* To whom correspondence should be addressed. Tel: +44 1603 255258. Fax: +441603 507723. E-mail: peter.wilde@bbsrc.ac.uk.

10.1021/jf050129y CCC: $30.25 © 2005 American Chemical Society
Published on Web 04/30/2005

mechanisms underlying fat crystallization in emulsion systems. Another important issue is to be able to routinely measure the physical properties of the fat droplets in emulsions during storage and use in order to optimize the production and storage process for maximal performance. To this end, we have made some preliminary investigations using densitometry and electron paramagnetic resonance (EPR) to validate them as potential techniques for monitoring of the development of fat crystals as a function of storage conditions in emulsion droplets.

BACKGROUND

The free radicals that we used as spin probes are 1,1,3,3-tetramethylisoindolin-2-yloxyl (TMIO) (mainly fat but also water soluble)

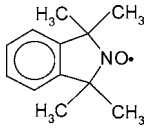

and the *n*-hexyl ester of 5-carboxy-1,1,3,3-tetramethylisoindolin-2-yloxyl (HCTMIO), which is only fat soluble.

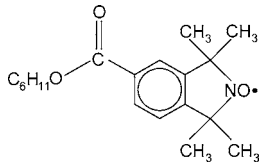

The general synthetic procedures and EPR properties of the probes have been described before (*16*−*19*). Partitioning experiments using *n*-octanol/water showed that the solubility of TMIO in water is <0.1%.

Nitroxyl radicals undergoing rapid rotational motion in an isotropic medium have their spectral anisotropy completely averaged. The corresponding EPR spectrum is characterized by three equally spaced lines having 1:1:1 intensities arising from hyperfine interactions of the nitrogen-14 nucleus with the unpaired electron. The widths of the lines can be accounted for by the motional modulation of the *g*-factor and the hyperfine interaction tensors. The rate of tumbling can be determined from the Lorentzian line widths, provided that the correlation time is less than 1 ns. Two rotational correlation times, $\tau_c(B)$ and $\tau_c(C)$, can be calculated using eqs 1 and 2 given below (*20*−*22*):

$$\tau_c(B) = 15B/(4b\Delta B_0) \quad (1)$$

$$\tau_c(C) = 8C/(28.02 \times 10^6 b^2) \quad (2)$$

where B_0 is the magnetic field at the center of the spectrum and the constants b and Δ can be found from the anisotropic hyperfine interactions and *g*-factors for the radicals. For TMIO type radicals, the equations become

$$\tau_c(B) = 5.75\ \{[W(-1) - W(+1)]/B_0\} \times 10^{-7}\ s \quad (3)$$

$$\tau_c(C) = 1.72\ \{[W(+1) + W(-1) - 2W(0)]\} \times 10^{-9}\ s \quad (4)$$

where $W(+1)$, $W(-1)$, and $W(0)$ are the peak-to-peak Lorentzian line widths of the first derivative EPR lines. A comparison of $\tau_c(B)$ and $\tau_c(C)$ tells us whether the spin probe is undergoing isotropic rotation, in which case, the ratio of the two correlation times must be close to unity. The rotational correlation time $\tau_c(B)$ corresponds to averaging of the three anisotropic hyperfine interactions and the three anisotropic *g*-values, whereas $\tau_c(C)$ only reflects the averaging of the hyperfine interactions. Ideally, both have the same value, but in general, calculation of $\tau_c(B)$ is more reliable than that of $\tau_c(C)$ and has been used in this work. Plots of $\ln\tau_c(B)$ or $\ln\tau_c(C)$ against the reciprocal of the absolute temperature should produce straight lines, whose slopes provide the activation enthalpy. If two parallel lines are obtained, then the radical can be regarded as undergoing isotropic motion. The TMIO type radicals used here have been shown to rotate essentially isotropically. Rotational correlation times, τ, are related to the viscosity, η, by the expression:

$$\tau = 4\pi r^3 \eta/3kT \quad (5)$$

where r is the effective radius of the spin probe, k is the Boltzman constant, and T is the absolute temperature. Other than in a neat liquid, η is the viscosity of the environment of the spin probe, that is, the microviscosity. This may be different from the bulk or macroviscosity of a complex fluid, which is measured on a larger length scale and will be influenced by networks or microstructures, which may form at longer length-scales than the spin probe.

Although EPR has been used before to study fat crystallization in emulsions (*23*), analysis was based on a simple relationship with peak height. Now, improved analysis is available to give more accurate information on the physical state of the oil droplets. This involved simulation and measurement of spectral parameters carried out using the EWVOIGTN computer program supplied by the Scientific Software Services (Bloomington, IL): The program is based on a precision fast convolution algorithm optimized by using a Levenberg−Marquardt method (*24*). This iterative fitting program enables a^N, *g*-values, Lorentzian and Gaussian line widths, and relative concentrations to be evaluated from EPR spectra resulting from overlap of spectra of two nitroxyl species. For the experiments with TMIO as a spin probe, two superimposed EPR spectra are observed originating from the water and lipid phases. These two overlapping spectra can be deconvoluted using the EWVOIGTN program, and this is easier to do when the two nitroxyls have different nitrogen hyperfine splittings (a^N) and/or different Lorentzian line widths. This situation occurs for oil/water emulsions because a^N is about 1.6 mT for a polar phase, whereas for the apolar phase a^N is about 1.4 mT (*25*).

MATERIALS AND METHODS

Sample Preparation. Emulsions were prepared from 28% hard palm kernel oil (HPKO), 71% water, 1% sodium caseinate, and 0.2% xanthan. HPKO contains the following fatty acids.

	%		%		%		%
lauric	47	oleic	14	caprylic	6	stearic	2.5
myristic	16	palmitic	8	capric	4	linoleic	2.5

HPKO is a soft solid at room temperature. The purpose of the protein is to form a layer around the oil droplets and to decrease the interfacial tension between the oil and the water phases: The emulsion is stabilized by a decrease in surface free energy.

Macroviscosity Measurements. The macroviscosity of HPKO was measured by stress viscometry using a model CS10 Bohlin controlled rheometer (Bohlin Instruments, Cirencester, United Kingdom) and a double gap GG 40/50 geometry at different temperatures from 323 to 353K. The shear rates were varied between 1.62 and 583 s^{-1} depending on viscosity of the sample and temperature used. The samples behaved

Table 1. Mean Viscosity Values of HPKO Measured between Shear Rates of 1.62 and 583 s^{-1} as a Function of Temperature[a]

temp (K)	viscosity (Pa.s)
323	2.14E–02 (1.46E–04)
333	1.59E–02 (5.51E–04)
343	1.24E–02 (1.12E–03)
353	1.02E–02 (1.29E–03)

[a] Mean (SD); $n = 75$. Viscosity was Newtonian between these shear rate values at all temperatures.

in a Newtonian manner at these shear rates, and the average viscosity values of this range were taken. These data were used to calculate the enthalpy of activation associated with the macroviscosity: This is the magnitude of the slope of an Arrhenius plot of ln(viscosity) vs *T*.

Density Measurements. An Anton Paar DMA 5000 density meter (Anton-Paar GmbH, Graz, Austria) was used to measure densities of the emulsions at controlled temperatures from 278 to 323K. The instrument uses an oscillating tube filled with the sample of interest and utilizes the principle of harmonic oscillation. The oscillating U-tube has a resonant frequency that is inversely proportional to the square root of its mass. Therefore, when filled with a liquid of known volume (approximately 1 mL), the mass, and hence the density, can be measured very accurately. It is estimated that errors are less than 10^{-4} g cm^{-3} for the emulsions used in this work. As the fat crystallizes in the emulsion, its density increases, enabling a direct measure of the overall levels of crystallized fat in the emulsion. The small sample volume means that the temperature can be changed and controlled quickly and accurately (±0.001 °C). The emulsions were heated to 323 K for 1 h to ensure that all of the fat was in the liquid state. The densities of the samples were recorded at intervals of 2.5 K on a cooling and subsequent heating cycle between 323 and 278 K at approximately 0.5 K per minute. Dynamic measurements were made by again heating the sample to 323 K, then cooling to a predetermined temperature (283, 288, or 293 K), and monitoring the density of a period of time to determine the rate crystallization of the oil in the emulsion.

EPR Measurements. Microcrystals of the spin probes were mixed into the emulsions to give a resultant probe concentration of about 1 mM. This concentration is appropriate for EPR measurements and is unlikely to affect the physical properties of the emulsions. Experiments were also carried out on neat HPKO. Samples were placed in 10 cm long glass capillary tubes (1 mm internal diameter), and the ends were heat sealed. X-band EPR spectra were recorded with a Bruker Elexys 500 spectrometer (Bruker Biospin Ltd., Coventry, U.K.) fitted with an ER049X Super X microwave bridge and a SHQ cavity: Variable temperature experiments were carried out with the aid of an ER131VT nitrogen controller. Spectra were processed off-line.

RESULTS AND DISCUSSION

Macroviscosity Measurements. The macroviscosity values of the HPKO as a function of temperature are shown in **Table 1**. The enthalpy of activation calculated from the macroviscosity measurements gave a value of 25.2 ± 0.9 kJ mol^{-1}.

Melting Point Measurements on HPKO. HPKO melting point data (provided by the suppliers of HPKO) have shown a wide range of temperatures due to it being a complex mixture of triglyceride molecules. The melting behavior at a heating rate of 2 K min^{-1} showed main peaks at 300.4 and 305.4 K whereas crystallization (cooling at 2 K min^{-1}) showed two peaks at 294.7 and 299.0 K. The structure and physical properties of HPKO crystals depend on the cooling rate and temperature, and they may change with time due to Ostwald ripening even though the solid fat content remains constant (*5*). In addition, the strength of crystal−crystal bonds and the fat crystal network increase at temperatures below the fat melting point (*26*).

Density Measurements on the Emulsions. It may be seen from **Figure 1** that there is considerable hysteresis when an

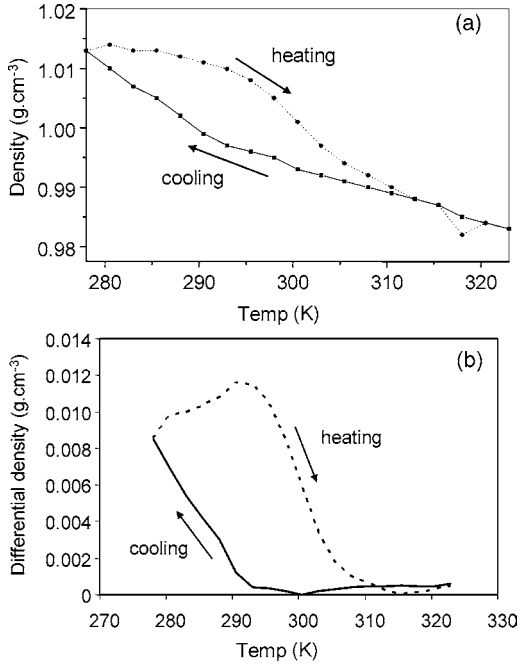

Figure 1. Effect of cooling (solid line) and heating (dashed line) on the density of the emulsion. (**a**) The absolute density values and (**b**) the differential density values compared with the density changes of the continuous phase.

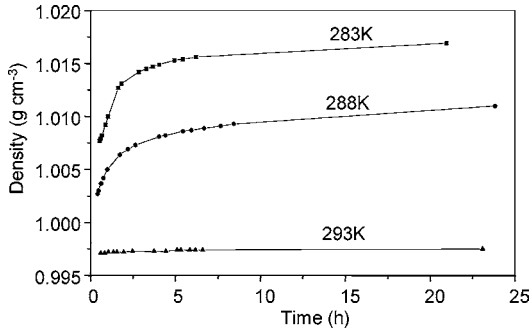

Figure 2. Effect of time on the density of the emulsion at various temperatures.

emulsion is gradually cooled from 323 to 278 K and then reheated to 323 K. The temperature of 323 K was chosen to ensure that the HPKO is liquid at the start of the experiment. The hysteresis in temperature is in the order of around 20 K, which is not uncommon in these systems. The rate of solidification was studied by again starting at 323 K and then dropping the temperature to 283, 288, and 293 K, in three separate experiments. From **Figure 2**, it can be seen that the density increases over a period of hours, being most marked for the lower temperatures. In fact, at 293 K, there was very little evidence of significant crystallization in the emulsions, whereas in the bulk oil, the fat would have already passed through its two main crystallization transition temperatures, resulting in significant solidification of the oil phase. This information is crucial for the performance of emulsions stored around this temperature. These results can be interpreted in terms of partial solidification of the HPKO over a fairly long interval.

The crystallization kinetics for HPKO in the bulk form can be very different from the emulsion form, which needs to be cooled to a much lower temperature in order for crystallization to start (*27*). In bulk oil, crystallization starts and nucleation and growth of the fat crystals rapidly extend throughout the whole system. However, when crystallization takes place in one

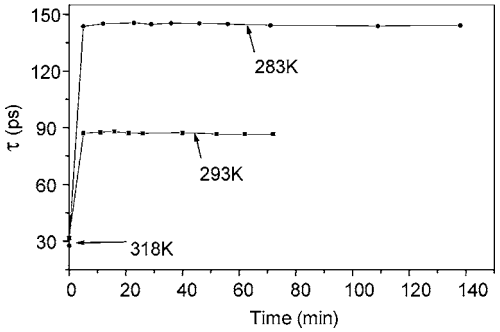

Figure 3. Effect of time on rotational correlation times, τ(B), of TMIO in neat HPKO at 283 and 293 K.

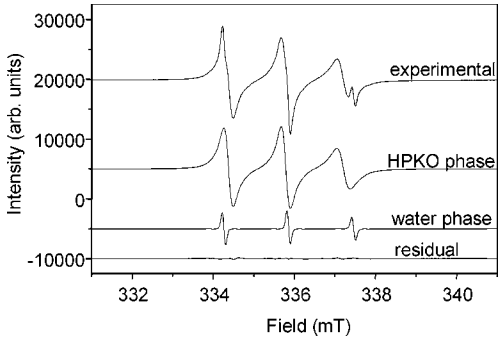

Figure 4. Deconvolution of the X-band EPR spectrum of TMIO in cream CA1 at 283 K.

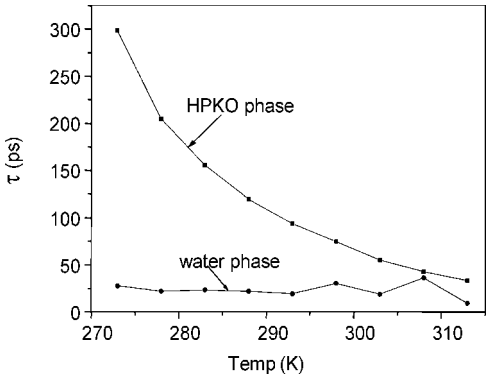

Figure 5. Effect of temperature on the rotational correlation times, τ(B), of TMIO in the HPKO and water phases of the cream CA1.

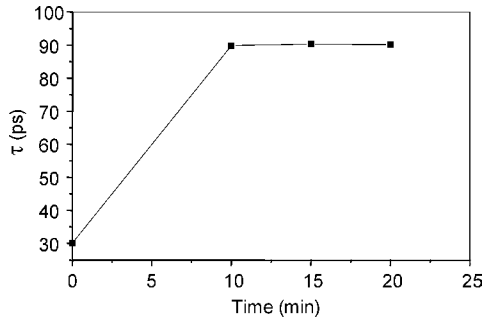

Figure 6. Effect of time on rotational correlation times, τ(B), of TMIO in cream CA1 at 293 K.

droplet of the emulsion, it cannot simply extend to the oil in the surrounding droplets (*5*). Several views occur as to why crystallization processes observed in the bulk fat are not seen in emulsified form (*7*). In commercial systems such as HPKO, impurities in the oil "seed" the nucleation of crystals, encouraging their growth. However, in small emulsion droplets, many of the droplets may not contain a nucleation site, so the process becomes more dominated by homogeneous nucleation and growth. Therefore, the temperature dependence and kinetics of crystallization in discrete emulsion droplets are very different to the bulk oil. Crystallization behavior of emulsified oil can depend on the mean size of the droplets (*13*), the type of emulsifier used (*28*−*30*), and the nature of the droplet−droplet interaction (*31*, *32*).

EPR Spectra of TMIO in HPKO. The EPR spectra of TMIO in neat HPKO were recorded over the temperature range 273−323 K; from the spectra, values of τ(B) were obtained in the range 25−250 ps. An Arrhenius plot was fitted linearly with $R = 0.9998$ giving an activation enthalpy of 34.7 ± 0.5 kJ mol^{-1}: Note that it was found that the enthalpy of activation obtained from macroviscosity measurements gives a value of 25.2 ± 0.9 kJ mol^{-1}. However, it is not uncommon for the microviscosity enthalpy to be greater than the macroviscosity enthalpy: This is because there is a small additional activation energy due to the spin probe being larger than the solvent molecules (*33*). A second series of experiments was carried out in which the bulk HPKO was held at 318 K and then dropped to 293 K and the spectra monitored at intervals for about 70 min, and the sample was heated to 318 K and then monitored at 283 K for about 140 min. It may be see from **Figure 3** that the rotational correlation times, τ(B), remain constant at 87.1 ± 0.5 and 144.7 ± 0.6 ps for 293 and 283 K, respectively, over the observation periods.

EPR Spectra of TMIO in the Emulsions. TMIO was added to a sample of the emulsion and EPR spectra recorded in 5 K intervals from 273 to 318 K. Because of the high water content and the significant solubility of TMIO in water, deconvolution of the spectra is very important. **Figure 4** shows an example of the experimental and deconvoluted spectra for 283 K. The spectral lines of TMIO in the HPKO phase are much broader than those in the water phase due to paramagnetic line broadening arising from dissolved oxygen; it has a much greater solubility in HPKO. From the deconvoluted spectra, it can be calculated that, due to the high solubility of TMIO in fat as compared with water, the partitioning of TMIO has a ratio of 28:1 for HPKO:water at 283 K; this compares with the ratio of HKPO:water of 0.39:1 used to make the emulsion. **Figure 5** presents the rotational correlation data obtained from the deconvolution computations. An Arrhenius plot for τ(B) values of the HPKO phase gives a linear plot ($R = 0.999$) yielding an activation enthalpy of 38.1 ± 0.6 kJ mol^{-1}, which is in reasonable agreement with the value obtained from the microviscosities of the neat HPKO. Comparison of **Figures 3** and **6** shows that at 283 and 293 K, the microviscosity of HPKO is slightly greater in the emulsion than it is in neat HPKO.

The values of τ(B) for the water phase do not show a smooth dependence on temperature due to computational errors. Nevertheless, there is a small increase of τ(B) from 313 to 273 K: A large change would not be expected because the enthalpy of activation for the macroviscosity of water is small having a value of only 17.23 ± 0.05 kJ mol^{-1} (*34*).

A set of experiments was carried out in which the emulsion was heated to 318 K and then cooled to 293 K and the EPR spectra were recorded over time; then, the temperature was raised to 318 K, cooled to 283 K, and again monitored over time. The spectra were deconvoluted, and values of τ(B) were obtained. There was no change observed at 293 K (**Figure 6**), but τ(B) increased with time at 283 K, as can be seen in **Figure 7**, from about 150 ps to about 200 ps over 140 min. This corresponds to an increase of microviscosity from about 15 centipoise to about 20 centipoise.

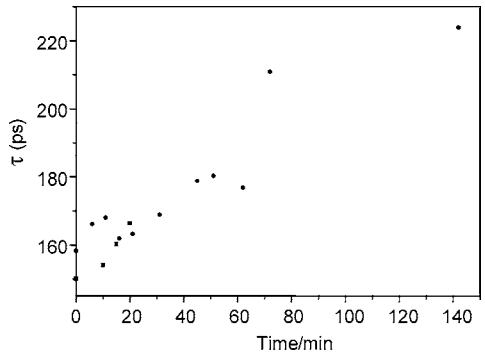

Figure 7. Effect of time on rotational correlation times, τ(B), of TMIO in cream CA1 at 283 K.

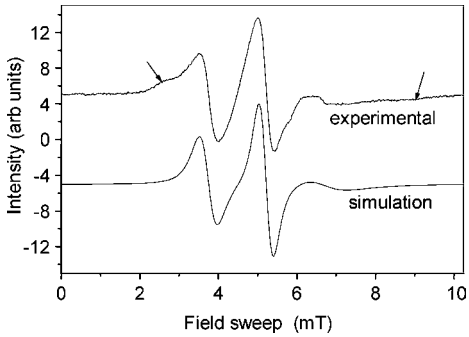

Figure 8. Experimental and simulated EPR spectra of HCTMIO in CA1 at 275 K after storage overnight at 273 K. The arrows indicate spectral features from a low mobility component.

There is some evidence that the time required to cool the cream to 283 K can affect the functional qualities. An experiment was carried with TMIO in the emulsion where the sample was cooled as quickly as possible from 318 to 283 K; in another experiment, the sample was cooled from 318 K in 1 K steps every 90 s until 283 K was reached. EPR spectra were recorded when 283 K was reached; τ(B) values of 141 ± 3 and 137 ± 5 ps, respectively, were obtained. Thus, there were no detectable differences in the microviscosities measured for the two types of cooling procedures.

HCTMIO Spin Probe Experiments. To reduce the computational complexities from having two phases to deal with, the fat soluble spin probe, HCTMIO, was used. There is a slight disadvantage in using this probe because it is larger than TMIO thus giving broader EPR lines resulting from a larger rotational correlation time. A key experiment was to attempt to see if aggregates of HPKO formed at low temperatures and HCTMIO is more suitable than TMIO for this purpose. A sample of emulsion was kept at 273 K overnight and then allowed to warm slowly with EPR spectra being recorded at intervals. From **Figure 8**, it may be seen that there is a low mobility component at 275 K. By subtracting the simulated from the experimental spectrum, the percentage of immobile to mobile component can be calculated. This was done at intervals as the temperature was raised. **Figure 9** shows how the amount of the low mobility component decreases as the temperature is raised; it should be noted that because of the errors in the estimation, concentrations below 5% are not regarded as significant. The simulated spectra in this experiment can be used to determine the rotational correlation time, τ(B), at the various temperatures. The data are shown in **Figure 10**. Note that the values of τ(B) for HCTMIO are about five times larger than those of TMIO under similar conditions, owing to the larger size of the probe.

In conclusion, density and EPR measurements are potentially useful and accessible tools for monitoring the physical properties

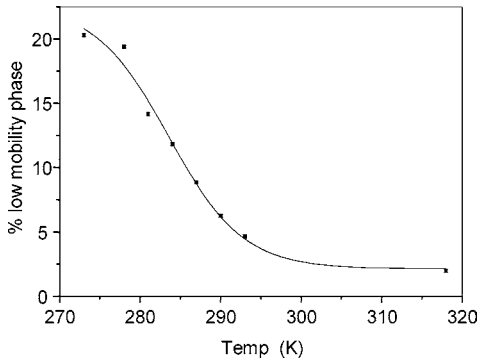

Figure 9. Effect of temperature on the percentage of the low mobility component in the emulsion after storage overnight at 273 K.

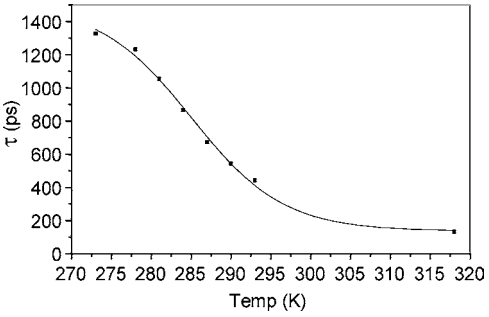

Figure 10. Effect of temperature on τ(B) calculated from the simulated spectra of HCTMIO in the emulsion after storage overnight at 273 K.

of emulsified oil droplets. Microviscosity values could provide an important insight into the properties of oil/fat droplets required for optimal functionality. Density measurements can provide a sensitive measure of the onset of crystallization, particularly under storage conditions close to the melting/crystallization temperatures of the oil, which could vary depending on other parameters such as droplet size and emulsifier type.

ACKNOWLEDGMENT

We thank Drs. S. E. Bottle and A. S. Micallef of Queensland University of Technology for the gift of HCTMIO.

LITERATURE CITED

(1) Dickinson, E.; Stainsby, G. *Colloids in Foods*; Applied Science: London, 1982.
(2) Rousseau, D. *Food Res. Int.* **2000**, *33*, 3.
(3) Boode, K.; Walstra, P.; De Grootmostert, A. E. A. *Colloids Surf., A* **1993**, *81*, 139.
(4) Granger, C.; Barey, P.; Combe, N.; Veschambre, P.; Cansell, M. *Colloids Surf., B* **2003**, *32*, 353.
(5) Dickinson, E.; McClements, D. J. In *Advances in Food Colloids*; Dickinson, E., McClements, D. J., Eds.; Blackie Academic & Professional: United Kingdom, 1995; pp 211−246.
(6) Goff, H. D. *Int. Dairy J.* **1997**, *7*, 363.
(7) Coupland, J. N. *Adv. Colloid Interface Sci.* **2002**, *7*, 445.
(8) Skoda, W.; Van den Tempel, M. *J. Colloid Sci.* **1963**, *18*, 568.
(9) Kloek, W.; Walstra, P.; van Vliet, T. *J. Am. Oil Chem. Soc.* **2000**, *77*, 643.
(10) Mutoh, T. A.; Nakagawa, S.; Noda, M.; Shiinoki, Y.; Matsumura, Y. *J. Am. Oil Chem. Soc.* **2001**, *78*, 177.
(11) Campbell, S. D.; Goff, H. D.; Rousseau, D. *Food Res. Int.* **2002**, *35*, 935.
(12) Higami, M.; Ueno, S.; Segawa, T.; Iwanami, K.; Sato, K. *J. Am. Oil Chem. Soc.* **2003**, *80*, 731.

(13) McClements, D. J.; Dungan, S. R.; German, J. B.; Simoneau, C.; Kinsella, J. E. *J. Food Sci.* **1993**, *58*, 1148.
(14) Hindle, S.; Povey, M. J. W.; Smithy, K. *J. Colloid Interface Sci*. **2000**, *232*, 370.
(15) Kalnin, D.; Garnaud, G.; Amenitsch, H.; Ollivon, M. *Food Res. Int*. **2002**, *35*, 927.
(16) Bolton, R.; Gillies, D. G.; Sutcliffe, L. H.; Wu, X. *J. Chem. Soc., Perkin Trans. 2* **1993**, 2049.
(17) Bolton, R.; Sutcliffe, L. H.; Wu, X. *J. Labelled Compd. Radiopharm.* **1994**, *XXXIV*, 663.
(18) Gillies, D. G.; Sutcliffe, L. H.; Wu, X. *J. Chem. Soc., Faraday Trans.* **1994**, *90*, 2345.
(19) Bottle, S. E.; Gillies, D. G.; Hughes, D. L.; Micallef, A. S.; Smirnov, A. I.; Sutcliffe, L. H. *J. Chem. Soc., Perkin Trans. 2* **2000**, 1285.
(20) Marsh, D. In *Spin Labeling. Theory and Applications*; Berliner, L. J., Reuben, J., Eds.; Academic Press: New York, 1989; pp 255−304.
(21) Fairhurst, S. A.; Pilkington, R. S.; Sutcliffe, L. H. Rotational correlation times and radii of dithiazol-2-yl and dithiazolidin-2-free radicals. *J. Chem. Soc., Faraday Trans. 2* **1983**, *79*, 439−452.
(22) Nordio, P. L. *Spin Labeling. Theory and Applications*; Berliner, L. J., Ed.; Academic Press: New York, 1976; pp 5−52.
(23) Mikhalev, O. I.; Karpov, I. N.; Kazarova, E. B.; Alfimov, M. V. *Chem. Phys. Lett.* **1989**, *164*, 96.
(24) Smirnov, A. I.; Belford, R. L. *J. Magn. Reson. B* **1995**, *103*, 65.
(25) Owenius, R.; Engström, M.; Lindgren, M.; Huber, M. *J. Phys. Chem. A* **2001**, *105*, 10967.
(26) Johansson, D.; Bergenstahl, B. *J. Am. Oil Chem. Soc.* **1995**, *72*, 911.
(27) Hodate, Y.; Ueno, S.; Yano, J.; Katsuragi, T.; Tezuka, Y.; Tagawa, T.; Yoshimoto, N.; Sato, K. *Colloids Surf., A* **1997**, *128*, 217.
(28) McClements, D. J.; Dickinson, E.; Dungan, S. R.; Kinsella, J. E.; Ma, J. G.; Povey, M. J. W. *J. Colloid Interface Sci.* **1993**, *160*, 293.
(29) Palanuwech, J.; Coupland, J. N. *Colloids Surf., A* **2003**, *223*, 251.
(30) Awad, T.; Sato, K. *Colloids Surf., B* **2002**, *25*, 45.
(31) McClements, D. J.; Dungan, S. R. *J. Colloid Interface Sci.* **1997**, *186*, 17.
(32) Vanapalli, S. A.; Palanuwech, J.; Coupland, J. N. *Colloids Surf., A* **2002**, *204*, 227.
(33) Pilãr, J. Private communication.
(34) Berstad, D. A.; Napstad, B. K.; Lamvik, M.; Skølsvik, P. A.; Tørklep, K.; Oye, H. A. *Physica* **1988**, *A151*, 246.

Received for review January 19, 2005. Revised manuscript received April 4, 2005. Accepted April 6, 2005. We thank Macphie of Glenbervie and BBSRC for financial support.

JF050129Y